An Adaptive LLC-Based and Hierarchical Power-Aware Routing Algorithm

Cesare Alippi, *Fellow, IEEE*, Romolo Camplani, and Manuel Roveri

Abstract—In a wireless sensor network (WSN), we can rarely assume the static network topology hypothesis. In fact, the topology may change due to unit and communication faults, energy availability, and environmental dynamics—situations that could prevent the acquired data to be successfully routed to the base station (BS). In recent years, many self-organizing routing algorithms that provide topology adaptation in an energy-aware context at the network level have been proposed. Among these, hierarchical algorithms are particularly adequate solutions for their scalability, power efficiency, extended network lifetime, and intrinsic adaptability abilities. This paper suggests a k-level hierarchical extension of the Low-energy Localized Clustering (LLC) algorithm that takes into account the estimate of the residual energy of nodes, the aggregation degree, and uniform coverage level of the monitoring area as well as extended lifetime for the network nodes. The effectiveness of the proposed solution has been validated with an ad hoc simulator and experimental investigations.

Index Terms—Distributed wireless measurement systems, energy management, power-aware routing algorithms, wireless sensor networks (WSNs).

I. INTRODUCTION

IN REAL-WORLD applications based on a wireless sensor network (WSN) technology, units generally live in a harsh highly dynamic environment, requiring the network to change over time to face permanent or transient node faults, failures, and environmental changes (e.g., a terrain landslide and presence of growing vegetation). Moreover, we can experience some units to run out of power with a subsequent unwished disconnection from the network; for some others, the opposite holds in the sense that units, back with energy, need to be reconnected. Finally, energy harvesting mechanisms [1]–[4] induce the network topology to change with an unpredictable dynamism.

In current deployments, since a fully reliable communication (e.g., see [5]–[7]) protocol is generally not addressed due to the power consumption overhead, acquired data are sent with a best effort modality, and unreceived measurements are lost data.

Development of smart routing algorithms is, hence, a must for assuring effective communications in large-scale WSNs, with adaptation ability being the key issue combined with

energy-aware aspects. In this direction, source-initiated [8] routing algorithms are excellent candidates due to their intrinsic ability to adapt to changing situations; however, in their traditional form, they cannot be accepted due to complexity and high power consumption issues [9]–[11].

To solve this aspect, self-organizing routing algorithms have been specifically developed for WSNs, which assure adaptability to environmental changes by providing a quick reaction to topological modification at the network level. In addition, they support an easy add-on and removal modality for nodes and reduce the energy consumption at the network level defined as the sum of residual energies of nodes [12]. Here, the specific literature suggests low-energy adaptive clustering hierarchy (LEACH) [13], localized clustering (LC) [14], Low-energy Localized Clustering (LLC) [15], hybrid energy-efficient distributed clustering algorithm [16], and Min Max D-Cluster [17].

These energy-aware algorithms share a common basic philosophy: The network is partitioned into clusters each ruled by a *cluster head* connected to its units with a star topology. Each cluster head is then directly connected to the base station (BS) and sends retrieved data through a single-hop communication mechanism. Since the network is organized without any hierarchy, the communication power delimits the coverage area; this limitation can be overcome with a multihop algorithm linking the cluster head levels.

In this paper, we propose the X-LLC algorithm, which extends LLC by considering a k-level tree-based hierarchy for the sensor nodes. The algorithm aims at guaranteeing a more uniform deployment of the nodes over the monitored area and prolonging their lifetime. Sensor nodes send data to the first-level cluster heads, which, in turn, forward them together with their own acquisitions to upper level cluster heads; the process iterates up the kth level, where cluster heads send all data directly to the BS. Nodes and cluster heads might consider a data aggregation phase to further reduce power consumption in transmission.

The presence of intermediate levels between simple nodes and BS reduces the energy consumption of the network since shorter transmission distances associated with multiple levels of cluster head mean lower transmission energy.

In the suggested algorithm, the identification of clusters and election of cluster heads is performed with a simple—yet effective—low-power distributed algorithm that provides the network with high adaptability to the changing environment.

Differently from the existing literature, we also take into account both a more precise estimate of the residual energy of a node by relying on supercapacitors as a storage mean and the

effects posed by imperfect aggregation of sensor data and the finite node-bandwidth.

The structure of this paper is given as follows. Section II briefly introduces and contrasts the LEACH, LC, and LLC routing algorithms. Section III presents the suggested extension to LLC with the multilevel hierarchical architecture encompassing aggregation degree, power consumption, and load balancing constraints. Experimental results are given in Section IV.

II. HIERARCHICAL ROUTING ALGORITHMS FOR WSNs

LEACH, LC, and LLC are cluster-based routing algorithms designed to assure scalability, power efficiency, and long system lifetime. They are generally characterized by the following three independent phases.

1) *Election*: nodes communicate with neighbors to dynamically establish cluster heads.
2) *Association*: neighborhood information is used to generate a hierarchical tree-based communication structure where leaves are the nodes and the root of the tree is the BS.
3) *Data communication*: sensor data are sent to the BS through the tree-based structure.

A. LEACH

In the election phase, the jth active node generates a random number η between 0 and 1. The node is an elected cluster head when η is smaller than the time-varying threshold h_j. We have

$$h_j = \begin{cases} \frac{P}{1-P(r \bmod (1/P))}, & \text{if the } j\text{th active node} \in G \\ 0, & \text{otherwise} \end{cases} \quad (1)$$

where r is the election round over time, P represents the expected percentage of cluster heads out of the available units and is fixed *a priori* by the network's designer, and G is the set of nodes that did not become a cluster head in the last $1/P$ election rounds.

Once elected, cluster heads broadcast an advertisement message to contact simple nodes in their neighborhood and wait for their answers. (Note that the neighborhood for a cluster head is defined by its fixed communication power.)

Each node decides to which cluster it will belong based on the signal power associated with the "reachable" cluster heads, i.e., a node selects the strongest—in terms of the received power—cluster head.

Cluster heads then generate and send a time-division multiple-access (TDMA) table to cluster nodes. At the end of the association phase, which implies *de facto* generation of a new network topology, nodes are ready to operate: data are acquired from sensors and are forwarded to the cluster head according to the defined TDMA table.

The main limitation of this algorithm is that the number of nodes composing a cluster differs from cluster to cluster since clusters are not balanced: some cluster heads coordinate a very large number of nodes where others do not.

B. LC

In LC, all nodes start the election phase by broadcasting an initial advertisement message according to a predefined communication power. Then, each node sets the internal *timer* with a value inversely proportional to the residual energy of the node and the number of received advertisements: the fewer the advertisement messages or the residual energy, the longer the countdown.

A node that terminates the countdown without receiving a message becomes a cluster head and sends an advertisement message to its neighbors that will interrupt the countdown and label themselves as nodes. Simple nodes belong to a cluster based on the received signal power, i.e., the preference is given to closer cluster heads since less transmission power is required. Khan *et al.* [15] has shown that LC guarantees good quality clusters and assures all nodes of the network to be reachable; isolated nodes become cluster heads. The main drawback of LC is the communication overhead associated with the advertisement messages of the election phase.

C. LLC

LLC reduces LC overhead by imposing a maximum value x on the percentage of nodes that can become a cluster head with x set at design time. The probability that node j is considered in the election phase at time t_r is proportional to its residual energy e_j [15], i.e.,

$$p_j = \frac{e_j tx}{e(t - t_r)} \quad (2)$$

where e is the initial energy of the node, and t is the expected network lifetime. Differently from LEACH, which relies on the concept of election round, LLC works on elapsed time. Probability p_j has the same role of the threshold h_j in LEACH.

All nodes not involved in the election phase wait for an advertisement message from elected cluster heads and subscribe to the one with the strongest received signal power.

D. Main Limitations of LEACH, LC, and LLC

Unfortunately the knowledge of the residual energy of nodes, which is necessary in LC and LLC, is rarely available. Moreover, LEACH, LC, and LLC assume perfect aggregation (i.e., the amount of data that a node has to forward does not exceed the amount of received data), but such a hypothesis for nodes is far from being true in real-world applications.

In addition, we might encounter situations where some nodes are not connected to the BS. This happens for those cluster heads whose distance from the BS is above the maximum reachable distance R_{MAX}.

Fig. 1(a) shows an example of an unreachable subnetwork (white circle), whereas Fig. 1(b) shows how the problem can be solved with a multihop solution. This phenomenon may arise in LEACH and LLC, as shown in [15]. However, it can be solved by modifying the protocols as follows: after the election phase, unreachable nodes have to connect directly to the BS. We should comment that in general, the probability that a node is not connected to the network is very low, while the probability
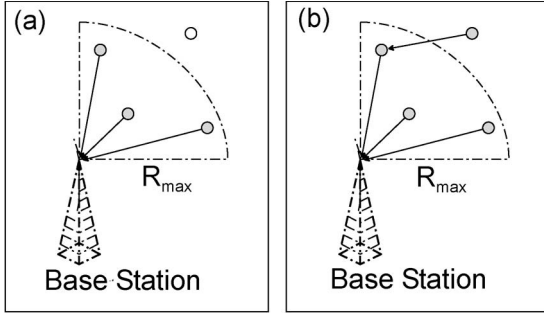
Fig. 1. (a) Single-hop network: a unit is unreachable. (b) Multihop network: each sensor is connected to the BS.
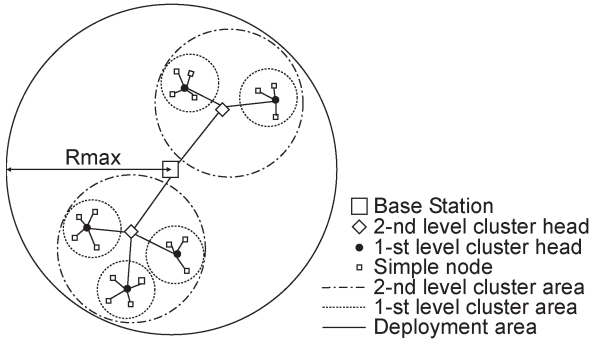
Fig. 2. X-LLC, $k = 2$.

that it will be reconnected in subsequent elections is high. Buffering mechanisms must be considered to avoid data losses in unreachable nodes.

As a last note, selection of the algorithm parameters might be critical. In fact, some parameter configurations proposed for LEACH, LC, and LLC, such as cluster heads percentage or expected network lifetime, are not realistic for most applications due to the unknown topology of the deployment. These aspects will be addressed in the following section.

III. k-LEVEL LLC

In this section, we extend LLC to a k-level hierarchical algorithm (see Fig. 2) to improve network energy management. Selection of LLC derives from the fact that it generally outperforms LEACH and LC in terms of the network lifetime, as attested in the literature [15], [18] and as also verified in Section IV describing our simulation experiments.

A. Setup Model

First, we make the following assumptions.
1) Antennas generate an isotropic spherical electromagnetic field [13].
2) The BS is central in the environment to better exploit communication coverage.
3) Nodes are uniformly distributed within the deployment area with density δ; under this assumption, δ times a given surface provides the expected number of units deployed in it.

Denote by P_w and R_w the wth power level and the associated transmission radius, respectively. Since the number of power

levels W in commercial units is fixed (e.g., around 8-10), we have that $P_w < P_{w+1}, \forall w \in 1, \ldots, W - 1$ from which $R_w < R_{w+1}$. The maximum transmission power arises for $P_W = P_{\mathrm{MAX}}$ with an associated $R_W = R_{\mathrm{MAX}}$ according to the first-order radio model and the free space assumption.

The expected number of nodes within the reachable environment is $N_0 = \delta \pi R_{\mathrm{MAX}}^2$; for larger networks, the above holds for each subnetwork communicating each other with a multihop communication protocol.

B. X-LLC: The Proposed Routing Algorithm

A k-level clustering hierarchy is particularly effective in reducing the energy consumption of the network compared to LLC since it allows for a short-range transmission activity. Moreover, it assures adaptability to changes that affect both the network and the environment and is autonomous in the routing decision. The former result derives from the fact that it automatically provides quick reactions to topological changes in the network by instructing new clustering configurations; the latter is a consequence of the fact that the routing algorithm is not centralized and nodes perform local decisions to select the optimal route.

Election Phase: Here, we consider $k \geq 1$ levels of cluster heads and k distinct election and association phases; LLC derives by selecting $k = 1$. Fig. 2 shows an example of a hierarchical structure.

Algorithm 1 *electClusterHeads*: i, n_{ji}
1. $m = 0$;
2. $u = rand\{U(0,1)\}$;
3. **if** $p_{ji} \geq u$ **then**
4. $\quad enableTimer(\tau_a)$;
5. $\quad send(msg_{ADV}, R_w)$;
6. $\quad$ **while** $isNotExpired(\tau_a)$ **do**
7. $\quad\quad$ **if** $receiveMessage(msg_{ADV})$ **then**
8. $\quad\quad\quad m = m + 1$
9. $\quad\quad$ **end if**
10. $\quad$ **end while**
11. **else**
12. $\quad sleepUntilElectionFinishes()$
13. $\quad$ **return**
14. **end if**
15. $\tau_b = calculatePromotionTimer\ (m, e_{ji})$
16. $enableTimer(\tau_b)$
17. **while** $isNotExpired(\tau_b)$ **do**
18. $\quad$ **if** $receiveMessage(msg_{ADV})$ **then**
19. $\quad\quad sleepUntilElectionFinishes()$
20. $\quad\quad$ **return**
21. $\quad$ **end if**
22. **end while**
22. $send(msg_{ADV}, R_w)$;

The suggested X-LLC algorithm is given in Algorithm 1, and the nomenclature of used symbols is provided in Table I.

In more detail, in step 1, each node initializes the number of advertisement messages received by a candidate node m at 0 and generates a uniformly distributed random value u between

TABLE I
SYMBOLS USED IN THE ALGORITHM

Symbol	Explication
N_0	Total number of nodes
S_i	the set of node sallowed to participate to the i-th level elections
n_{ji}	the j-th node $\in S_i$
e_{ji}	the residual energy of n_{ji} power level
p_{ji}	probability that n_{ji} participates to the election phase (compute with Eq. 2)
R_w	the transmission radius at the w-th transmission power level
τ_a, τ_b	the timer values of the node

0 and 1 (step 2) to be compared (step 3) with threshold p_{ji} defined in (2): if p_{ji} is above u, the node becomes a candidate cluster head and participates to the election phase; otherwise, it stays silent (step 12) until the election process terminates. The node timer is enabled in a countdown modality starting at value τ_a (step 4). Each candidate node broadcasts an advertisement message with transmission power P_w, which covers a spatial neighborhood of radius R_w. Then, each candidate node collects the advertisement messages coming from the other candidate nodes in the neighborhood (step 7) and counts the received messages by increasing m (step 8). When time τ_a expires, the candidate sets the promotion timer to τ_b (step 15); τ_b is function of the number of received messages m and the node residual energy. Finally, if τ_b expires, the candidate node becomes a cluster head at level i, and it broadcasts an advertisement message with transmission power P_w (step 23). Conversely, if the timer is still counting down and the node receives an advertisement message (step 18), it interrupts the promotion timer and waits the termination of the election process (step 19).

Cluster heads at level i participate to the $(i + 1)$th-level cluster heads election; if not elected, they simply remain cluster heads at level i.

Association Phase: The association phase starts after the completion of the election process and comprises k specific association subphases that are performed in a top-down fashion starting from the BS to simple nodes. In the first association phase, the kth-level cluster heads associate themselves to the BS, which sends them back the TDMA table. Then, the $(k - 1)$th-level cluster heads register to the nearest kth-level cluster head, which answers by providing the TDMA table; the process iterates down to the sensor node level.

X-LLC allows shrinking the cluster size by acting on the radius through the use of different power levels. This provides a remarkable advantage in terms of transmission energy consumption reduction with respect to (w.r.t.) traditional hierarchical algorithms.

Moreover, the following also hold true.

1) Each cluster head rules over a small number of nodes.
2) Cluster heads forward collected information to a cluster head at a higher abstraction level instead of sending them directly to the BS.
3) The transmission range of simple nodes can be reduced w.r.t. the one required by LLC. Consequently, transmission requires less power, and the intercluster interference decreases.
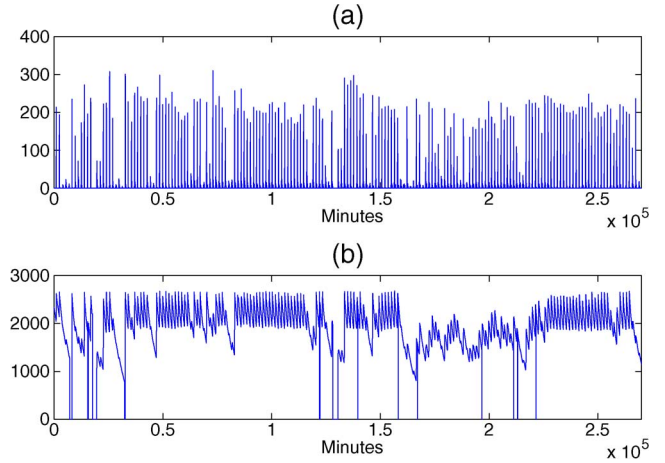
Fig. 3. (a) Solar power (in miliwatts) acquired by the solar panel. (b) Residual energy (in joules) in the supercapacitor measured according to (3).

Determination of the optimal number of levels for a given application depends on the characteristics of the deployment, the introduced overhead of the hierarchy, the type of nodes, the aggregation degree, the available bandwidth, and residual energy.

C. Efficient Node Energy Estimation

The knowledge of the energetic state of nodes is pivotal in the selected routing algorithms since the election phase is based on such information.

Unfortunately, the residual energy might be unavailable information since traditional energy storage means are batteries. In the best case, we can provide a rough estimate with accuracy decreasing with battery ageing. Moreover, the charge/discharge curve is nonlinear and time variant, and batteries require full discharge/recharge cycles to maximize their lifetimes. Optimal recharge cannot be granted during the operational life since the provided energy [e.g., through photovoltaic (PV) cells] is a nonconstant over time.

Instead, the residual energy can be estimated by considering supercapacitors [19] as storage means. In particular, the residual energy e_j can simply be evaluated as

$$e_j = \frac{1}{2}CV_j^2 \tag{3}$$

where V_j and C are the voltage of the supercapacitor of the jth unit and its equivalent capacitance, respectively. To evaluate the accuracy of the residual energy estimate, we considered an embedded unit [4] composed of a polycrystalline PV cell of nominal 0.5 W suitably connected to three supercapacitors in a series configuration ($C = 350$ F each). Fig. 3(a) shows the solar power acquired in a 55-day acquisition campaign. The residual energy in the supercapacitor is given in Fig. 3(b); units were acquiring, processing, and sending data 24 h per day.

The percentage difference between residual energy computed with (3) and the one actually stored in the supercapacitor is 4.56%. Availability of the residual energy estimate with high accuracy makes the use of X-LLC and energy-based algorithms effective.
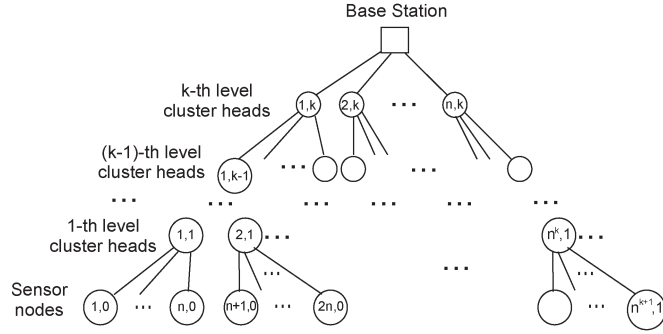
Fig. 4. Hierarchical balanced structure of the sensor network.

Fig. 5. Calculated throughput T_i w.r.t. level i when A ranges from 0 to 1 (step 0.25). $b_s = 1$ kb/s and $n = 5$.

D. Bandwidth Limitations

Let B_M and b_s be the maximum bandwidth (in kilobits per second) for each unit and the throughput (in kilobits per second) derived from the sensing activity, respectively.

By assuming that a 100-A% aggregation of the data received at each level is performed, the throughput of the ith-level cluster head is the sum of its own sensing activity b_s and the throughputs of the $(i-1)$th-level cluster heads associated to it multiplied by A. When $A = 1$, *no aggregation* is performed during routing, and the ith-level cluster heads forward their own sensing activity together with 100% of the data received from the $(i-1)$th cluster heads. On the contrary, $A = 0$ represents the *perfect aggregation* extreme.

Bandwidth limitations of each unit force the cluster heads throughput to be always smaller than B_M for each level.

In the particular case of WSNs organized as n-ary balanced trees (see Fig. 4), the relationship between throughput of the sensing activity and bandwidth limitations can be solved in closed form.

Each ith-level cluster head aggregates 100 A% of received data and forwards received data to its upper level cluster head together with the acquired data: the throughput of each ith-level cluster head is then $T_i = nAT_{i-1} + b_s$, where n is the ratio between the cluster heads of level $i-1$ and the cluster heads of level i. By induction, the throughput of ith-level cluster heads may be formalized as

$$T_i = b_s \frac{(nA)^{i+1} - 1}{nA - 1}. \tag{4}$$

Due to the hierarchical structure of the sensor network, T_i measures the traffic passing through each cluster head at level i. In other words, T_i represents the 100 A% aggregated sum of throughputs of all sensor nodes and lower level cluster heads of the subtree rooted in the ith level. Fig. 5 presents the influence of the parameter A on the throughput T_i. Obviously, when $A = 0$, T_i does not depend on i since its value is always b_s: in case of perfect aggregation, the cluster head forwards only its own acquisitions. The case $A = 1$ represents the highest throughput T_i achievable by the cluster heads at the ith level.

Since T_i is the throughput of the sensor units at the ith level, the network has to guarantee a suitable bandwidth to assure correct data transmission to the $(i+1)$th level. This critical issue has never been addressed by traditional hierarchical routing algorithms that assume perfect aggregation so that bandwidth limitation is no longer an issue.
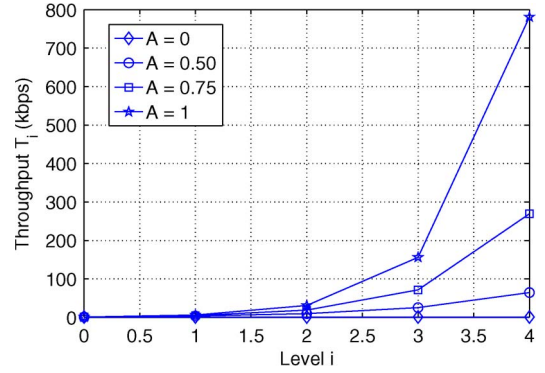
In a nonperfect aggregation case, the incoming bandwidth of the units of level i must be larger than the throughput of the units of level $(i-1)$: when this constraint is not satisfied, the network cannot work properly since packets may get lost before reaching the BS.

Without any loss of generality, let us assume that the network adopts a TDMA as a medium access control layer; this is a reasonable assumption, as also shown in [13]. Let b_0 (in kilobits per second) be the overhead in terms of bandwidth usage introduced by the synchronization message of the TDMA; the incoming bandwidth of cluster heads and BS is $B_M - b_0$.

In an n-ary balanced tree, the number of k-level cluster heads connected to the BS is n, and the maximum available outgoing bandwidth guaranteed by the BS is

$$B_k = \frac{B_M - b_0}{n}. \tag{5}$$

Starting from B_k, we can recursively identify the outgoing bandwidth available to cluster heads at level i as follows:

$$B_i = \frac{B_{i+1} - b_0}{n}, \qquad where \, 0 \leq i \leq k \tag{6}$$

which can also be expressed as

$$B_i = \frac{B_M}{n^{k-i+1}} - b_0 \frac{n^{k-i+1} - 1}{n^{k-i+1}(n - 1)}. \tag{7}$$

As intuitively stated, the outgoing bandwidth available to cluster heads increases with i. kth-level cluster heads have the largest $B = B_k$ bandwidth [from (5)], while sensor nodes assume the lowest value B_0.

The amount of available bandwidth w.r.t. the total number of levels (i.e., BS, k levels of cluster heads, and simple sensor nodes) for the most important commercial sensor units is listed in Table II, where $n = 5$, and $b_0 = 1$ kb/s. As expected, the available bandwidth decreases quickly with the increase of the number of levels. From the table, Micaz and Tmote support up to 5 levels (i.e., BS, $k = 3$ levels of cluster heads, and sensor nodes) with $b_s = 1$ kb/s, which represents a reasonable throughput in many environmental applications. Differently, Mica2 supports only four levels (i.e., BS, $k = 2$ levels of cluster heads, and the sensor nodes), while the Dot version can only be used with one level of cluster heads (i.e., LLC).

Fig. 6 presents the effect of the TDMA overhead b_0 on the available bandwidth; in this case, $n = 2$ and $B_M = 250$ kb/s.

TABLE II

AVAILABLE BANDWIDTH OF COMMERCIAL SENSOR UNITS W.R.T. THE TOTAL NUMBER
OF LEVELS (I.E., BS, k LEVELS OF CLUSTER HEADS, AND SENSOR NODES)

Available bandwidth (kbps)	Number of levels				
	2 ($k=0$)	3 ($k=1$)	4 ($k=2$)	5 ($k=3$)	6 ($k=4$)
Micaz, Tmote	250	49.8	9.76	1.75	0.15
Mica 2	38.4	7.4	1.28	0.05	0
Dot	10	1.8	0.16	0	0
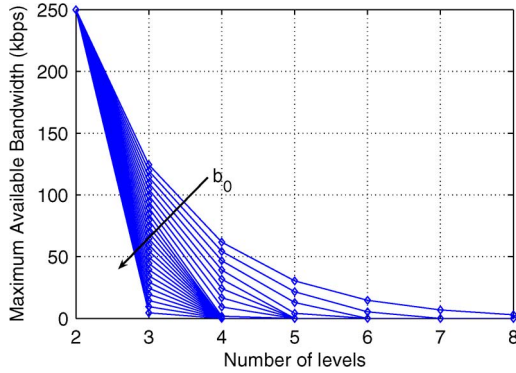
Fig. 6. Calculated maximum available bandwidth w.r.t. the number of levels for Micaz ($n = 2$ and $B_M = 250$). b_0 ranges from 1 to 250 kb/s.
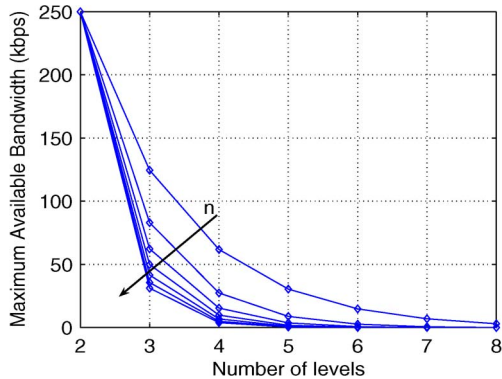
Fig. 7. Calculated maximum available bandwidth w.r.t. the number of levels for Micaz ($b_s = 1$ and $B_M = 250$). n ranges from 2 to 7.

The available bandwidth decreases as b_0 increases since the overhead reduces the bandwidth available for the transmission of acquired data. The effects of n over the available bandwidth is presented in Fig. 7. As expected from (6), the larger n is, the smaller the available bandwidth will be, which must be shared with a larger number of units.

E. Relationships Among Design Parameters

Under the assumed hypotheses, the node density of the ith-level cluster head is

$$\delta_i = \frac{n}{\pi R_i^2}. \tag{8}$$

Moreover, in the case of an n-ary balanced tree, the number of nodes n is not a function of the level number. Consequently, we get

$$\delta_i \pi R_i^2 = \delta_{i+1} \pi R_{i+1}^2$$

TABLE III

POWER CONSUMPTION FOR THE ELECTION AND ASSOCIATION PHASES

	Power consumption (mW)
LEACH	13.4
LC	13.2
LLC	9.5
X-LLC	17.9

from which

$$R_{i+1} = R_i \cdot \sqrt{\frac{\delta_i}{\delta_{i+1}}}. \tag{9}$$

Finally, from (8) and (9), we obtain

$$R_{i+1} = R_i \cdot \sqrt{n}. \tag{10}$$

Starting from the kth hierarchical level for which $R_k = R_{\mathrm{MAX}}$, (10) provides sequence R_i and, then, the transmission power needed at each level.

IV. SIMULATION RESULTS

At first, we measure the power consumption overhead of X-LLC, LEACH, LC, and LLC due to the election and association phases (Section IV-A) in a real deployment. Then, we simulate the performance of algorithms in terms of system lifetime, energy consumption, and live nodes distribution in the long run (Section IV-B).

A. Phase 1: Measuring the Power Consumption of the Election and Association Phases

We configured a WSN composed of 10 Mica2 units to measure the power consumption of the election and the association phases.

We fixed the packet size for advertisement and synchronization to 40 bits, the bandwidth to 38.4 kb/s (being Mica2), and $b_s = 1$ kb/s. We also assumed that each node sends a single data packet at each round and that $k = 2$ from Table II. Other parameters (e.g., R_i) have been determined according to (10). For LLC and LEACH, we considered the parameters suggested in [18] and [15], respectively.

The network evolved for 30 min, and the power consumption was measured. The average power consumption for the election and association phases are given in Table III.

We observe that LLC outperforms the other algorithms in terms of power consumption, while X-LLC consumes more due to the overhead associated with the hierarchical structure of the network. We believe that the double power consumption of X-LLC w.r.t. LLC is associated with the $k = 2$ choice since the computational complexity of X-LLC scales with k.

In line with [15], we observe that the power consumption of the election and association phases of LLC is lower than
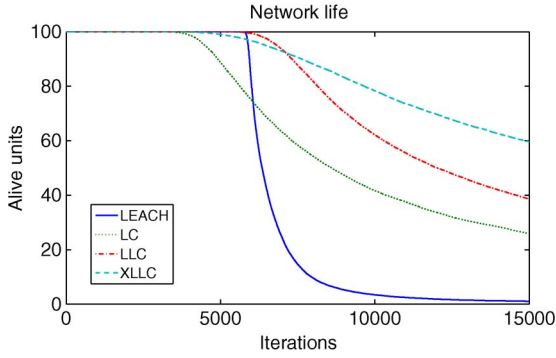
Fig. 8. Network liveness, $N_0 = 100$.
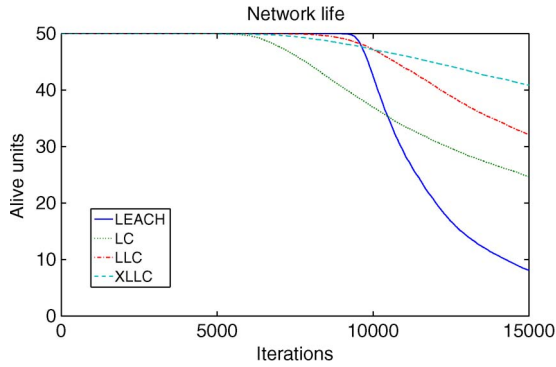
Fig. 9. Network liveness, $N_0 = 50$.

the ones of LC and LEACH. This is due to the fact that in LC, all units participate the election phase and, as such, send messages and wait for answers from elected cluster heads. Differently, LLC bounds the number of units that can undergo the election process. As far as LEACH is concerned, the higher power consumption is related to the fact that there is a non-null probability of having nodes not connected to cluster heads that require a direct connection to the BS. In turn, this implies a larger transmission range.

B. Phase 2: Simulating the System Lifetime, Energy Consumption, and Live Node Distribution

An ad hoc simulator was developed to evaluate the different performance in terms of system lifetime, energy consumption, and live nodes distribution on a large WSN in the long run. We uniformly deployed 100 and 50 units within a circular environment of radius $R_{\mathrm{MAX}} = 40$ m with the BS in the center. We considered a first-order radio model and the free space assumption: the energy loss is, hence, assumed to be proportional to R^2. Moreover, the message size for data is 1024 bits, and the advertisement and synchronization messages are 40 bits each. A generic node was charged with an initial energy $e = 1$ J, its bandwidth is 40 kb/s, and the sensor throughput $b_s = 1$ kb/s.

Each simulation iteration consists of data acquisition and transmission, while the election and the association phases are activated with a lower frequency, e.g., one election and association phase out of ten iterations.

Missing parameters (e.g., R_i) have been determined, as suggested in Section III; a $k = 2$ level hierarchy of cluster heads was selected for X-LLC.
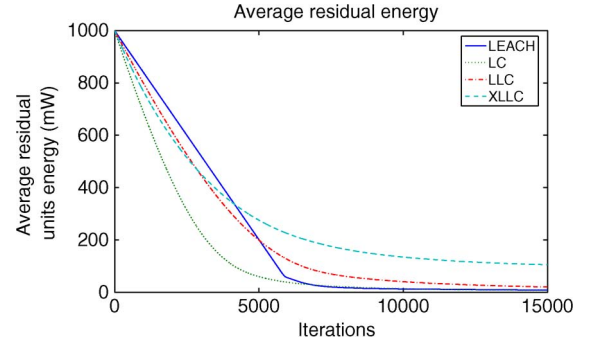
Fig. 10. Average residual unit energy, $N_0 = 100$.
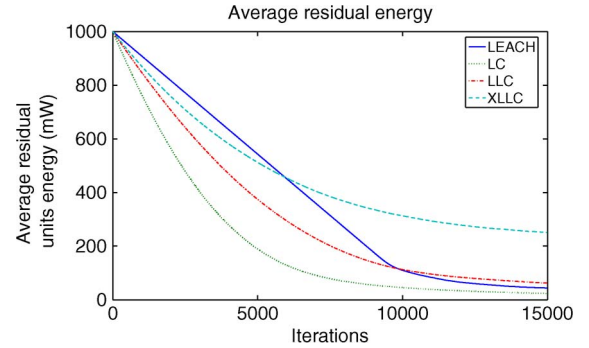
Fig. 11. Average residual unit energy, $N_0 = 50$.
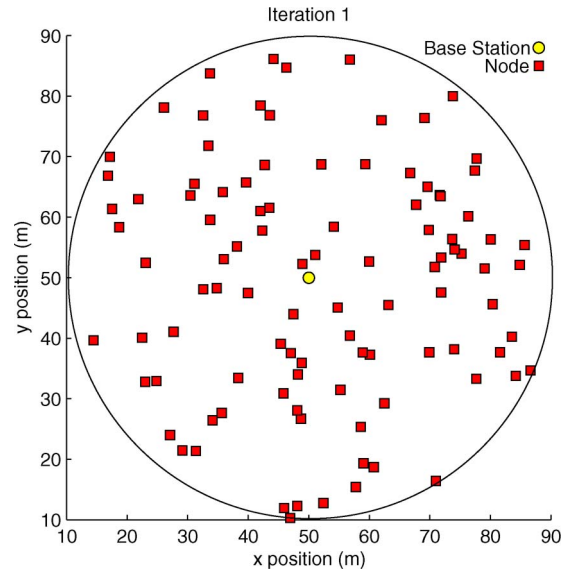
Fig. 12. Initial deployment of the units in the WSN.

We consider two figures of merit:
1) the network liveness, defined as the percentage of live units in a given iteration w.r.t. the initial ones;
2) the average residual unit energy, which is defined as

$$\frac{\sum_{j=0}^{N_{\mathrm{Tot}}(r)} e_j}{N_{\mathrm{Tot}}(r)} \quad (11)$$

where $N_{\mathrm{Tot}}(r)$ is the number of live units at iteration r, and e_j is the residual energy of the jth live unit.

Results regarding the network liveness are given in Fig. 8 ($N_0 = 100$) and Fig. 9 ($N_0 = 50$); the abscissa represents the
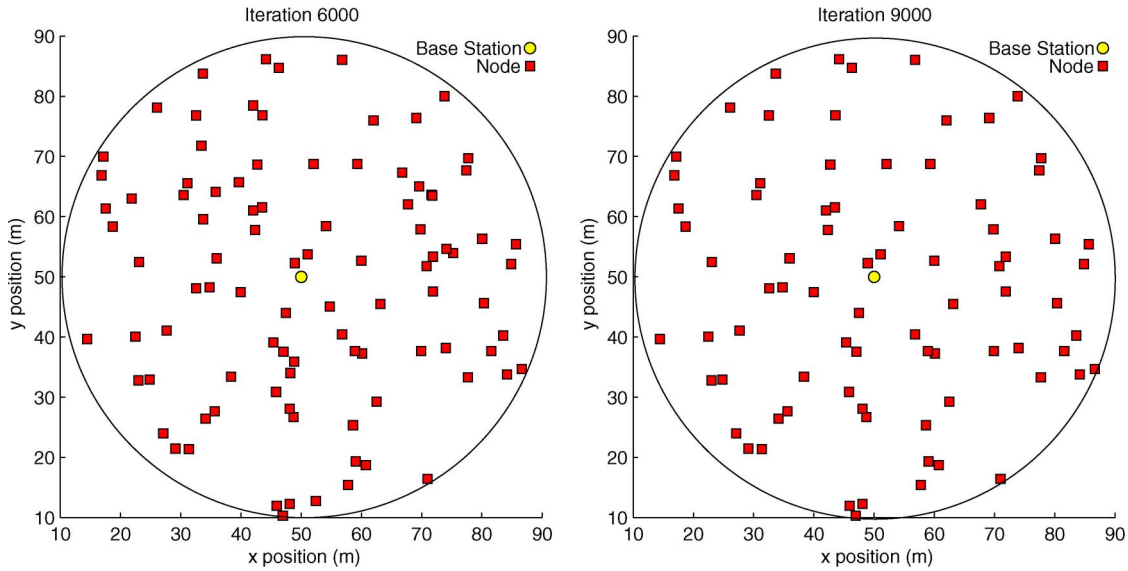
Fig. 13.   X-LLC: live units in the WSN at iterations 6000 and 9000.
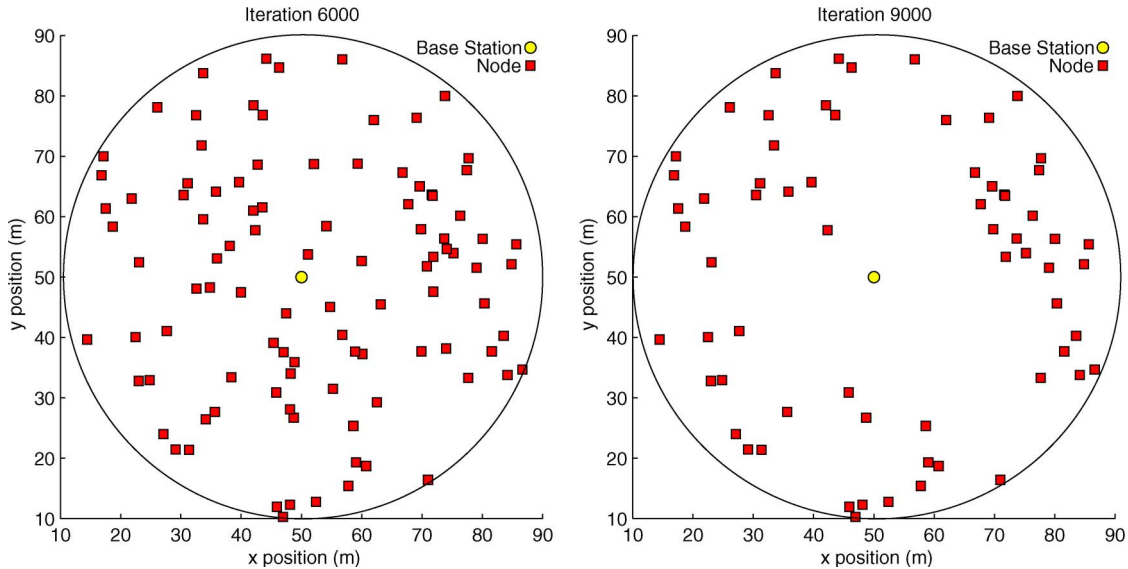
Fig. 14.   LLC: live units in the WSN at iterations 6000 and 9000.

simulation iterations, and the ordinate represents the number of alive units. Those regarding the average residual energy are given in Figs. 10 and 11.

We observe that LEACH outperforms, at the beginning, all other algorithms in terms of the number of alive units due to its immediate election phase, i.e., random election of cluster heads. However, the simplicity of the election phase in LEACH does not assure a balanced energy consumption of units at the network level. For this reason, most units run out of energy in the mid long run (see Figs. 8 and 9).

Differently, X-LLC consumes more at the beginning when many units are available, but it outperforms the others in the mid long run. This behavior can be explained by considering that the hierarchical structure generated during the association phase introduces a transmission overhead balanced by a reduced transmission range.

A uniform distribution for alive units is a desirable property that we would expect from an effective monitor-

ing system that considers all environmental areas of equal relevance.

The second advantage of X-LLC is that it assures a more uniform distribution of units, as verified in Fig. 12 for a WSN with $N_0 = 100$ units.

The network units evolve over time. Snapshots of the WSN configuration in correspondence with cases where $r = 6000$ and $r = 9000$ are given in Fig. 13 (X-LLC), Fig. 14 (LLC), Fig. 15 (LC), and Fig. 16 (LEACH). As expected, since no energy-harvesting mechanisms are present, units run out of energy and switch off. In particular, LLC, LC, and LEACH generate large empty monitoring areas in proximity to the BS due to the excessive usage of units there deployed, e.g., refer to the $r = 9000$ case.

The uniform distribution can be verified by evaluating the probability distribution of cluster heads at a given iteration r. In particular, we computed the probability $p_{CH}(R, R + \Delta, r)$ to find a cluster head in the $[R, R + \Delta]$ annular
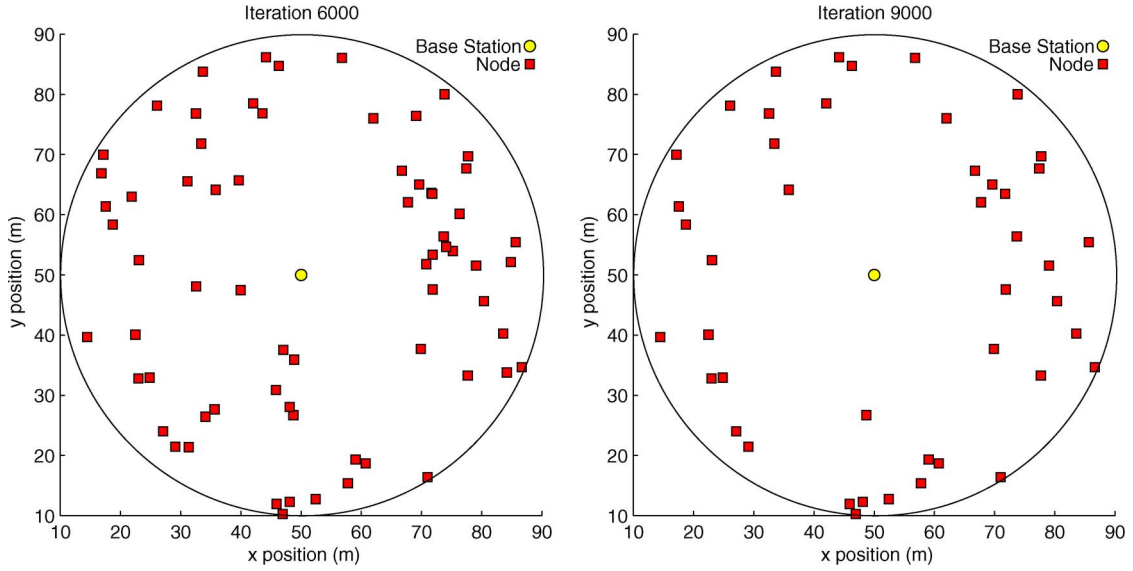
Fig. 15.   LC: live units in the WSN at iterations 6000 and 9000.
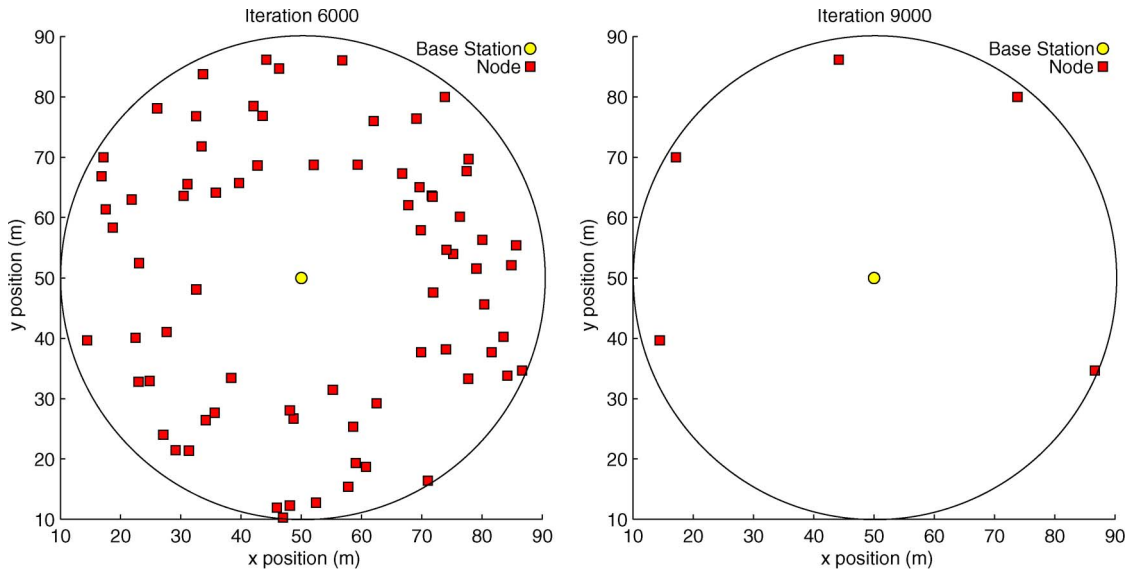
Fig. 16.   LEACH: live units in the WSN at iterations 6000 and 9000.

area identified by radii R and $R+\Delta$, $\Delta > 0$ from the BS, as follows:

$$p_{\mathrm{CH}}(R, R+\Delta, r) = \frac{\sum_{j=0}^{N_{\mathrm{Tot}}(r)} I_{d_j \in (R, R+\Delta)}}{N_{\mathrm{Tot}}(r)} \frac{1}{\pi(R+\Delta)^2 - \pi R^2} \tag{12}$$

where d_j is the Euclidean distance of the jth alive unit to the BS, and $I_{d_j \in (R, R+\Delta)}$ is the indicator function that assumes value 1 if the node belongs to the area, and 0 otherwise.

Figs. 17–20 show p_{CH} at iterations 1500, 4500, and 7500 for LEACH, LC, LLC, and X-LLC in the $N_0 = 100$ case, respectively. As expected, LEACH, LC and LLC gradually reduce the probability of electing cluster heads close to the BS. This effect is particularly evident at $r = 7500$, where $p_{\mathrm{CH}} \approx 0$ in the $(0, 20)$-m interval. On the contrary, X-LLC exhibits a

more uniform distribution of cluster heads, even in the long run, as can be appreciated by the distribution of p_{CH} over iterations.

In our opinion the more uniform distribution of live nodes in X-LLC, which has been experimentally evaluated, is due to a balanced energy consumption of units at the network level (please refer to Figs. 8 and 9 and related comments).

V. CONCLUSION

This paper has presented an extension of the LLC routing algorithm by introducing a hierarchical structure in the network management. Network units are clustered with a hierarchical approach, which, by exploiting the nature of the topology, allows us to improve adaptability, network lifetime, and over-head load balance among clusters. The novelty of the proposed approach resides in two main issues. First, a k-level hierarchical
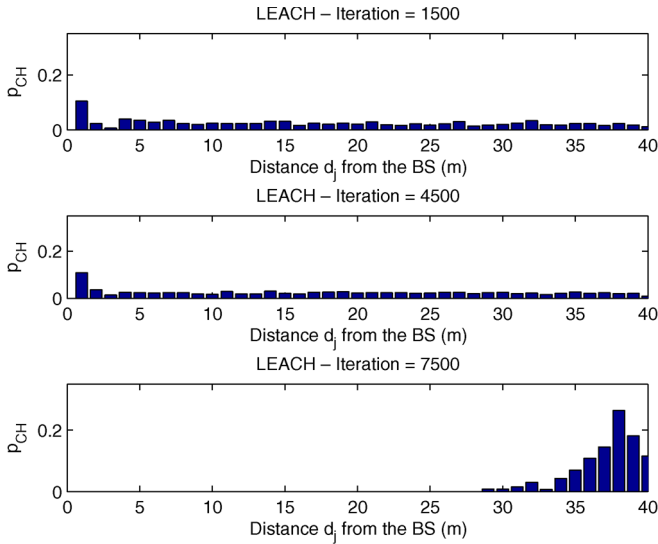
Fig. 17. Probability of finding a cluster head at iterations 1500, 4500, and 7500 with LEACH.
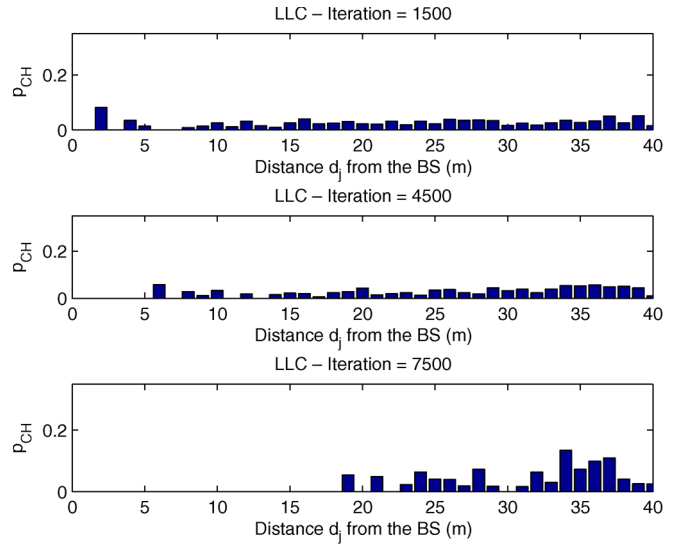
Fig. 19. Probability of finding a cluster head at iterations 1500, 4500, and 7500 with LLC.
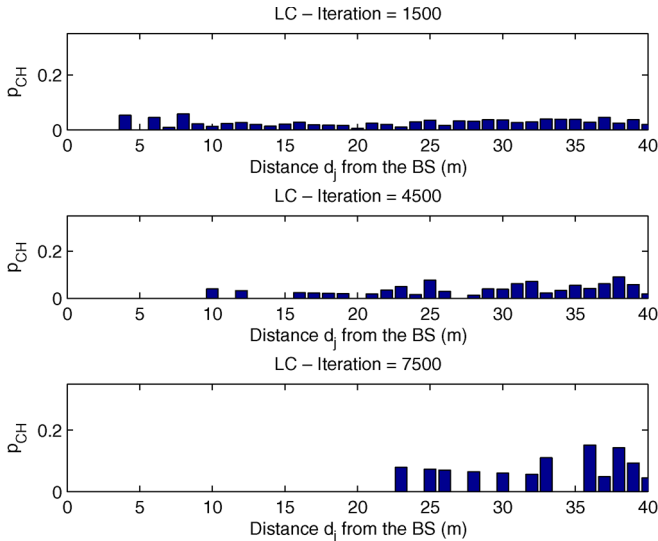
Fig. 18. Probability of finding a cluster head at iterations 1500, 4500, and 7500 with LC.
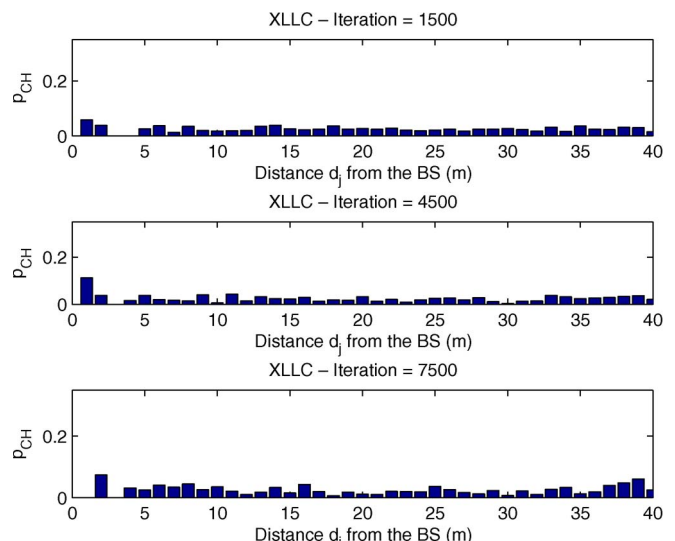
Fig. 20. Probability of finding a cluster head at iterations 1500, 4500, and 7500 with X-LLC.

structure of cluster heads is suggested, while the literature only considers one level of cluster heads. Second, the proposed solution is applicable for any degree of aggregation, while traditional algorithms assume perfect aggregation.

The suggested algorithm also provides a more uniform distribution of live nodes in the deployment area, which is an appealing feature since it allows receiving data all over the environment, even when the network is reducing its acquisition ability due to energy shortage.

election algorithm in X-LLC) greatly helped in improving the manuscript.

REFERENCES

[1] G. Ottman, H. Hofmann, A. Bhatt, and G. Lesieutre, "Adaptive piezoelectric energy harvesting circuit for wireless remote power supply," *IEEE Trans. Power Electron.*, vol. 17, no. 5, pp. 669–776, Sep. 2002.

[2] J. Paradiso and T. Starner, "Energy scaveging for mobile and wireless electronics," *Pervasive Comput.*, vol. 4, no. 1, pp. 18–27, Jan.–Mar. 2005.

[3] M. Rahimi, H. Shah, G. Sukhatme, J. Heideman, and D. Estrin, "Studying the feasibility of energy harvesting in a mobile sensor network," in *Proc. IEEE ICRA*, Taipei, Taiwan, Sep. 2003, pp. 19–24.

[4] C. Alippi and C. Galperti, "An adaptive system for optimal solar energy harvesting in wireless sensor network nodes," *IEEE Trans. Circuits Syst. I, Reg. Papers*, vol. 55, no. 6, pp. 1742–1750, Jul. 2008.

[5] P. Ferrari, A. Flammini, D. Marioli, and A. Taroni, "IEEE802.11 sensor networking," *IEEE Trans. Instrum. Meas.*, vol. 55, no. 2, pp. 615–620, Apr. 2006.

[6] P. Ferrari, A. Flammini, D. Marioli, A. Taroni, and E. Sisinni, "A Bluetooth-based sensor network with web interface," *IEEE Trans. Instrum. Meas.*, vol. 54, no. 6, pp. 2359–2364, Dec. 2005.

[7] Y. Kim, R. G. Evans, and W. M. Iversen, "Remote sensing and control of an irrigation system using a distributed wireless sensor network," *IEEE Trans. Instrum. Meas.*, vol. 57, no. 7, pp. 615–620, Jul. 2008.

[8] E. Royer and C.-K. Toh, "A review of current routing protocols for ad hoc mobile wireless networks," *IEEE Pers. Commun.*, vol. 6, no. 2, pp. 46–55, Apr. 1999.

[9] C. Perkins and E. Royer, "Ad-hoc on-demand distance vector routing," in *Proc. 2nd IEEE WMCSA*, New Orleans, LA, Feb. 1999, pp. 90–100.

[10] D. B. Johnson and D. A. Maltz, "Dynamic source routing in ad-hoc wireless networks," in *Mobile Computing*, vol. 353. New York: Springer-Verlag, 1996, pp. 153–181.

[11] V. D. Park and M. S. Corson, "A highly adaptive distributed routing algorithm for mobile wireless networks," in *Proc. IEEE INFOCOM*, Apr. 1997, pp. 1405–1413.

[12] K. Sha and W. Shi, "Modeling the lifetime of wireless sensor networks," *Sensor Lett.*, vol. 3, no. 2, pp. 126–135, 2005.

[13] W. Heinzelman, A. Chandrakasan, and H. Balakrishnan, "Energy-efficient communication protocol for wireless microsensor networks," in *Proc. 33rd Annu. Hawaii Int. Conf. Syst. Sci.*, Maui, HI, Jan. 2000, vol. 2, p. 10.

[14] D. Estrin, R. Govindan, J. Heidemann, and S. Kumar, "Next century challenges: Scalable coordination in sensor networks," in *Proc. 5th Annu. ACM/IEEE Int. Conf. Mobile Comput. Netw. (MobiCom)*, 1999, pp. 263–270.

[15] M. Khan, B. Bhargava, and L. Lilien, "Self-configuring clusters, data aggregation, and authentication in microsensor networks," Dept. Comput. Sci., Purdue Univ., West Lafayette, IN, Tech. Rep. CSD TR 03-003, Mar. 2003.

[16] O. Younis and S. Fahmy, "Heed: A hybrid, energy-efficient, distributed clustering approach for ad hoc sensor networks," *IEEE Trans. Mobile Comput.*, vol. 3, no. 4, pp. 366–379, Oct.–Dec. 2004.

[17] A. Amis, R. Prakash, T. Vuong, and D. Huynh, "Max–min D-cluster formation in wireless ad hoc networks," in *Proc. IEEE 19th Annu. INFOCOM*, Mar. 2000, vol. 1, pp. 32–41.

[18] I. Akyildiz, W. Su, Y. Sankarasubramaniam, and E. Cayirci, "Wireless sensor networks: A survey," *Comput. Netw.*, vol. 38, no. 4, pp. 393–422, Mar. 2002.

[19] B. E. Conway, "Transition from 'supercapacitor' to 'battery' behavior in electrochemical energy storage," in *Proc. 34th Int. Power Sources Symp.*, 1990, pp. 319–327.

Cesare Alippi (SM'94–F'06) received the Dr.Ing. degree (*summa cum laude*) in electronic engineering and the Ph.D. degree in computer engineering from Politecnico di Milano, Milan, Italy, in 1990 and 1995, respectively.

He has completed research work in computer sciences at the University College, London, U.K., and the Massachusetts Institute of Technology, Cambridge. He is currently a Full Professor of information processing systems with Politecnico di Milano. He is the author of more than 120 technical papers published in international journals and conference proceedings. His research interests include application-level analysis and synthesis methodologies for embedded systems, computational intelligence, and wireless sensor networks.

Dr. Alippi is an Associate Editor of the IEEE TRANSACTIONS ON NEURAL NETWORKS and the IEEE TRANSACTIONS ON INSTRUMENTATION AND MEASUREMENT.

Romolo Camplani received the Dr.Ing. degree in electronic engineering and the Ph.D. degree in electronic and computer science from Università degli Studi di Cagliari, Cagliari, Italy, in 2003 and 2008, respectively, and the M.Eng. degree in embedded system design from the Università della Svizzera Italiana, Lugano, Switzerland.

He is currently a Postdoctoral Researcher with Politecnico di Milano, Milan, Italy. His research interests include wireless sensors networks, adaptive routing algorithms, and power-aware embedded applications.

Manuel Roveri received the Dr.Ing. degree in computer science engineering and the Ph.D. degree in computer engineering from Politecnico di Milano, Milano, Italy, in June 2003 and May 2007, respectively, and the M.S. degree in computer science from the University of Illinois, Chicago, in December 2003.

He is a currently a Postdoctoral Researcher with Politecnico di Milano. His research interests include computational intelligence, adaptive algorithms, and wireless sensor networks.